Science Advances
AAAS

Supplementary Materials for

A phospho-tyrosine–based signaling module using SPOP, CSK, and LYN controls TLR-induced IRF activity

Kazuki Tawaratsumida *et al.*

Corresponding author: Hans Häcker, hans.haecker@path.utah.edu

Sci. Adv. **8**, eabq0084 (2022)
DOI: 10.1126/sciadv.abq0084

The PDF file includes:

Figs. S1 to S8

Other Supplementary Materials for this manuscript includes the following:

Table S1

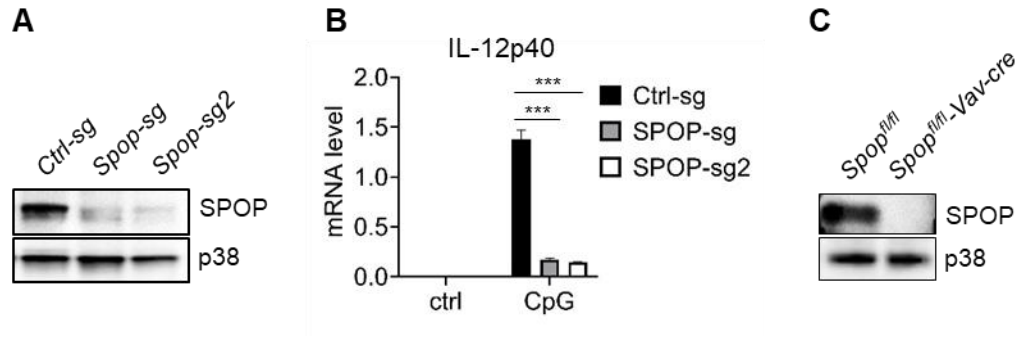

Fig. S1. Efficient deletion of *Spop* in RAW264.7 cells and splenocytes from *Spop*$^{fl/fl}$-*Vav-cre* mice.

(A) IB analysis of RAW264.7 cells expressing CAS9 that were transduced with vectors encoding control sgRNA (ctrl) and two independent *Spop*-specific sgRNAs (SPOP-sg and SPOP-sg2).

(B) Q-PCR analysis of RAW264.7 cells described in (A) that were stimulated with CpG-DNA for 4 h.

(C) Immunoblot analysis of lysates from splenocytes derived from *Spop*$^{fl/fl}$ and *Spop*$^{fl/fl}$*-Vav-cre mice.*

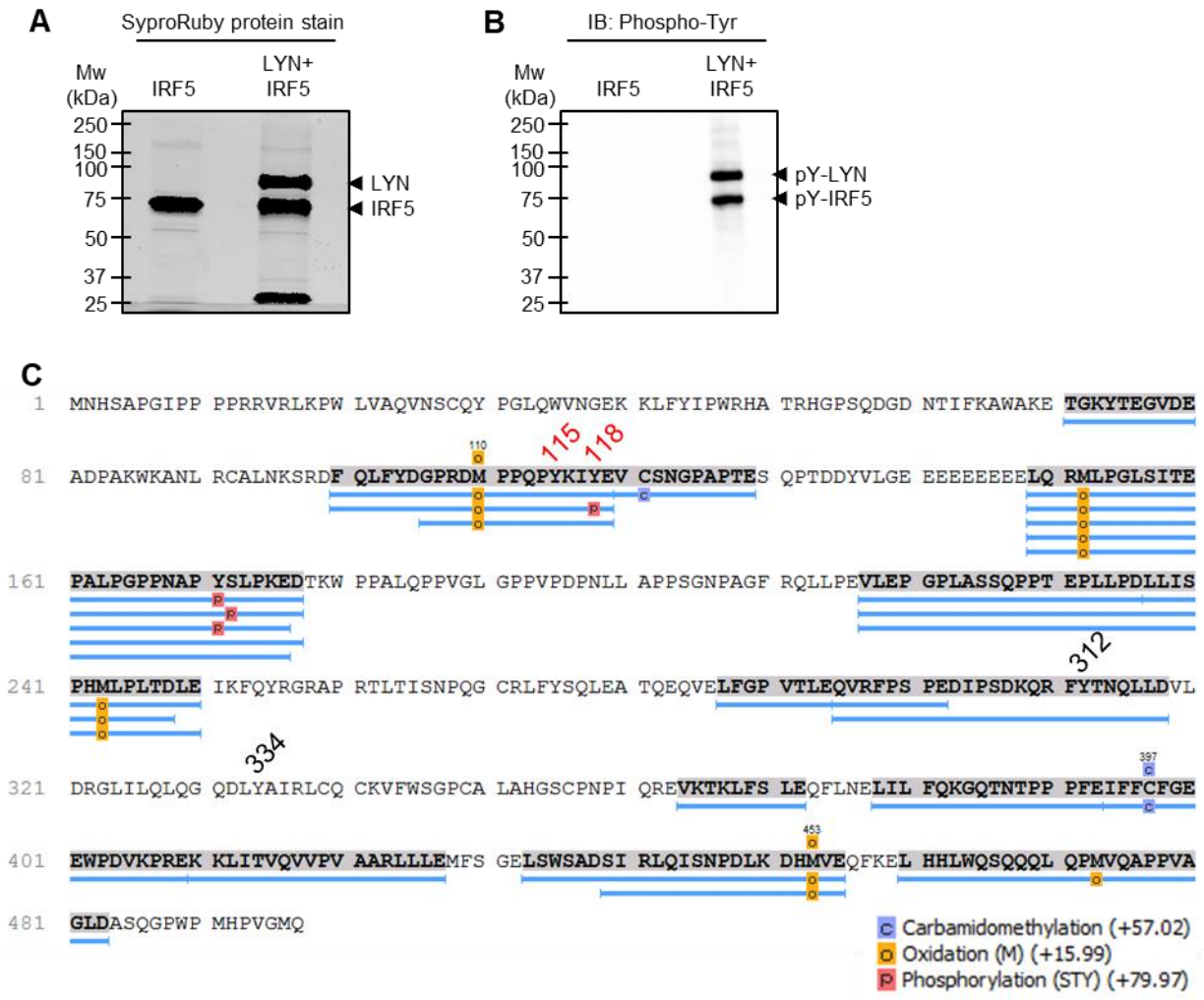

D

	digested by	phospho site
IRF5 w/o Lyn	Trypsin	S56, S157, S172, S286, T291,
IRF5 with Lyn	Trypsin	T75, Y171, S172, S445
IRF5 with Lyn	GluC	Y115 or Y118, Y171, S172,

Fig. S2. MS analysis of LYN-mediated in vitro phosphorylation of IRF5.
(A) SyproRuby-stained SDS PAGE of IRF5 and IRF5/ LYN after incubation for 1 hour to allow for LYN-mediated IRF5 phosphorylation.
(B) IB analysis of samples described in (A) using a phospho-tyrosine-specific antibody.
(C) IRF5 sequence with GluC-digest peptides and modifications identified by MS (blue lines). The Y115 and Y118 sites are highlighted in red. Phospho-peptides containing the Y118p residue (sequence in red) were identified based on 7 MS/MS scans (PSM=7) with the Y118-phospho-site assigned based on characteristic (y2, y3, (b18)2+, and (b19)2+) MS/MS fragment ions.
(D) Complete list of peptides containing phosphorylation sites identified by MS.

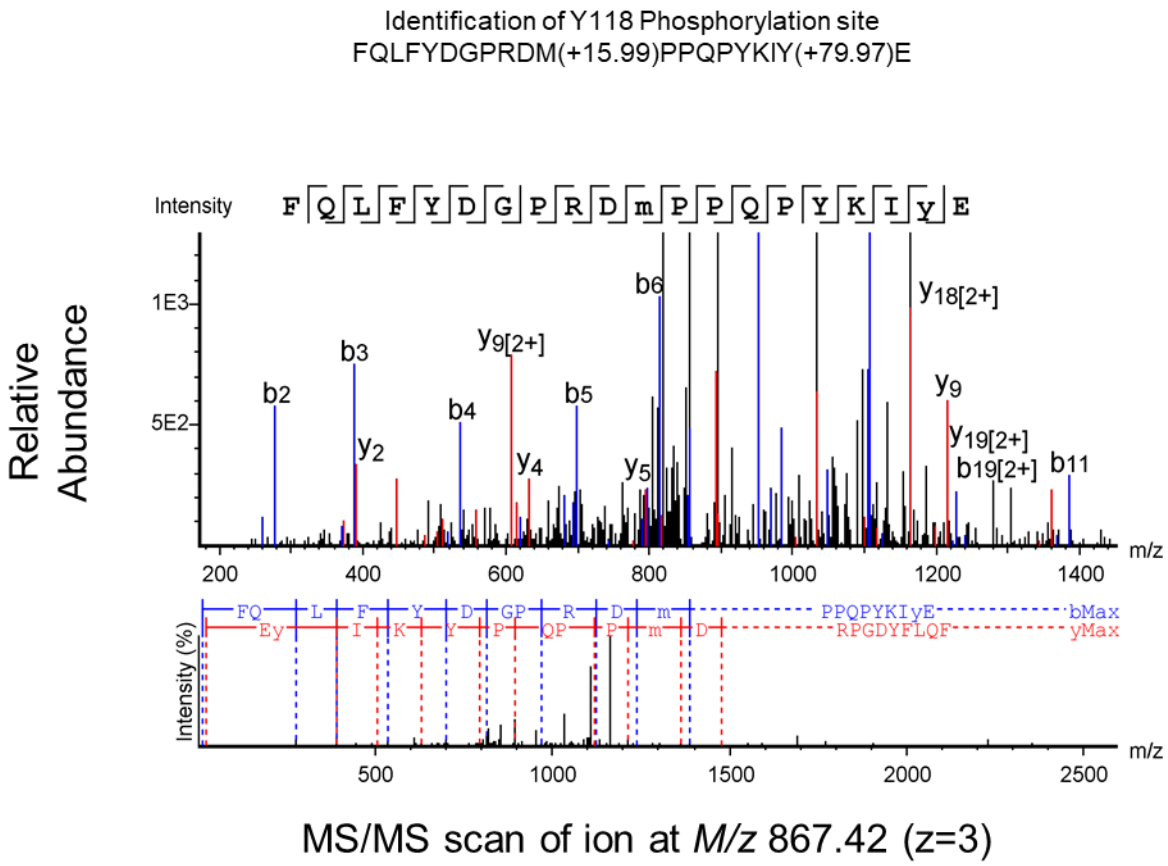

Fig. S3. MS/MS fragmentation data for Mouse IRF5 Aa 100-119 sequence (GluC-peptide). The peptide FQLFYDGPRDM(+15.99)PPQPYKIY(+79.97)E at M/z 867.42 (z=3) is presented, showing b/y ions. The Y118 phosphorylation site was assigned based on characteristic fragment ions at M/z 391.18 (y2), at M/z 504.12 (y3), at M/z 1105.71 [$(b18)^{2+}$], and at M/z 1227.26 [$(b19)^{2+}$].

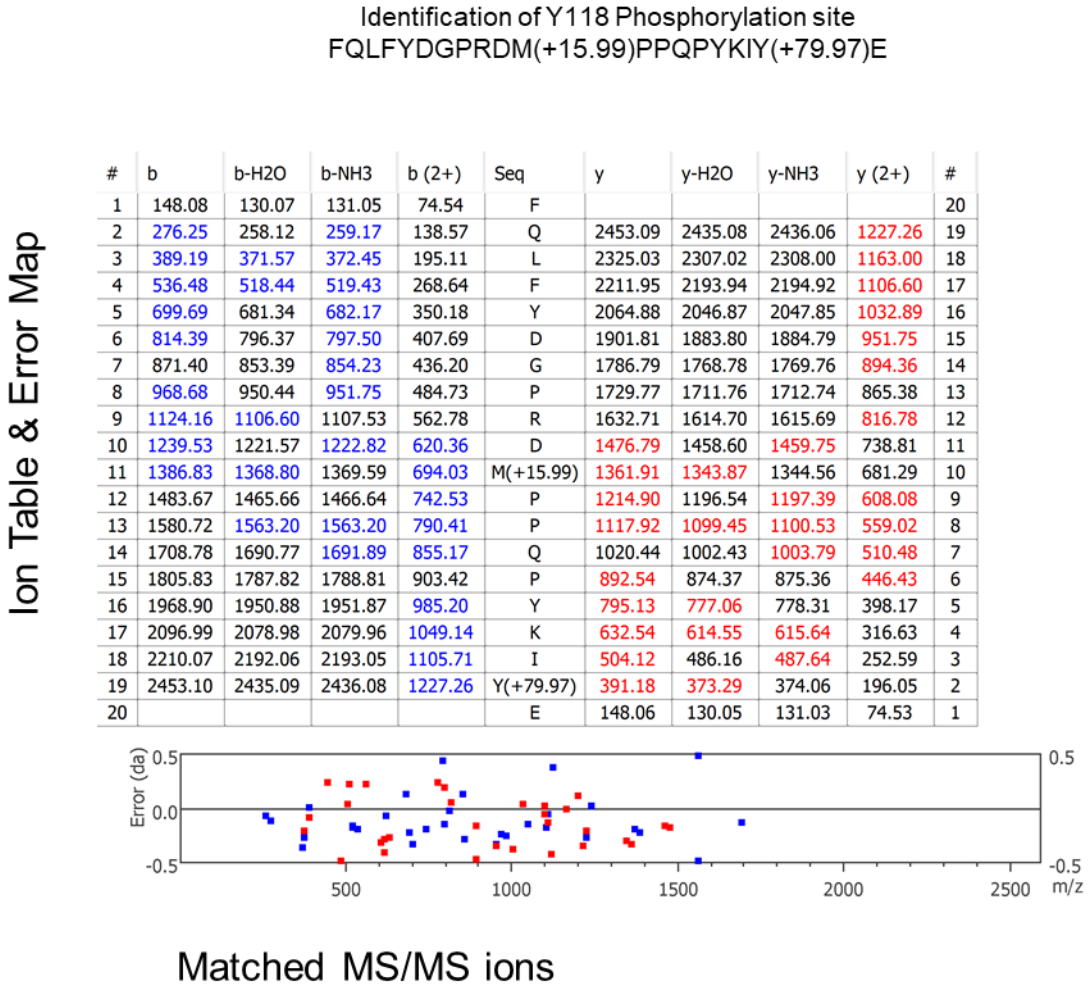

#	b	b-H2O	b-NH3	b (2+)	Seq	y	y-H2O	y-NH3	y (2+)	#
1	148.08	130.07	131.05	74.54	F					20
2	276.25	258.12	259.17	138.57	Q	2453.09	2435.08	2436.06	1227.26	19
3	389.19	371.57	372.45	195.11	L	2325.03	2307.02	2308.00	1163.00	18
4	536.48	518.44	519.43	268.64	F	2211.95	2193.94	2194.92	1106.60	17
5	699.69	681.34	682.17	350.18	Y	2064.88	2046.87	2047.85	1032.89	16
6	814.39	796.37	797.50	407.69	D	1901.81	1883.80	1884.79	951.75	15
7	871.40	853.39	854.23	436.20	G	1786.79	1768.78	1769.76	894.36	14
8	968.68	950.44	951.75	484.73	P	1729.77	1711.76	1712.74	865.38	13
9	1124.16	1106.60	1107.53	562.78	R	1632.71	1614.70	1615.69	816.78	12
10	1239.53	1221.57	1222.82	620.36	D	1476.79	1458.60	1459.75	738.81	11
11	1386.83	1368.80	1369.59	694.03	M(+15.99)	1361.91	1343.87	1344.56	681.29	10
12	1483.67	1465.66	1466.64	742.53	P	1214.90	1196.54	1197.39	608.08	9
13	1580.72	1563.20	1563.20	790.41	P	1117.92	1099.45	1100.53	559.02	8
14	1708.78	1690.77	1691.89	855.17	Q	1020.44	1002.43	1003.79	510.48	7
15	1805.83	1787.82	1788.81	903.42	P	892.54	874.37	875.36	446.43	6
16	1968.90	1950.88	1951.87	985.20	Y	795.13	777.06	778.31	398.17	5
17	2096.99	2078.98	2079.96	1049.14	K	632.54	614.55	615.64	316.63	4
18	2210.07	2192.06	2193.05	1105.71	I	504.12	486.16	487.64	252.59	3
19	2453.10	2435.09	2436.08	1227.26	Y(+79.97)	391.18	373.29	374.06	196.05	2
20					E	148.06	130.05	131.03	74.53	1

Fig. S4. Ion table displaying MS/MS fragmentation data for Mouse IRF5 Aa 100-119 (GluC-peptide).
The sequence FQLFYDGPRDM(+15.99)PPQPYKIY(+79.97)E at M/z 867.42 (z=3) is displayed, showing b/y ions. The Y118 phosphorylation site was assigned based on characteristic fragment ions at M/z 391.18 (y2), at M/z 504.12 (y3), at M/z 1105.71 [(b18)2+], and at M/z 1227.26 [(b19)2+].

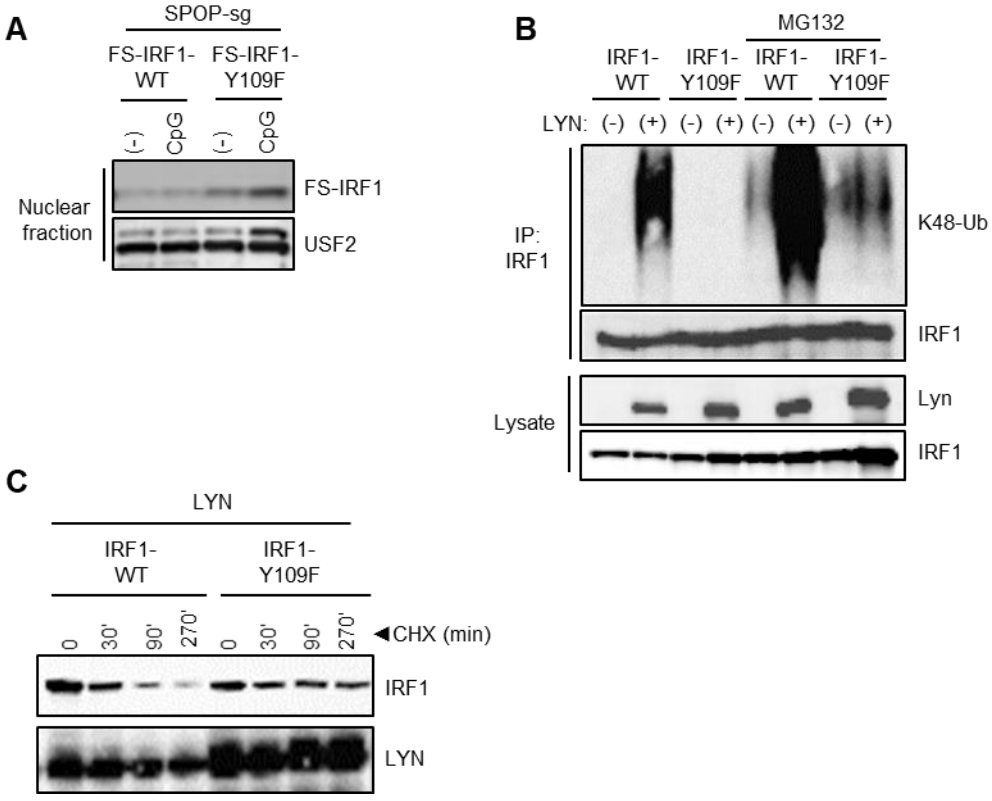

Fig. S5. The conserved tyrosine in IRF1 controls LYN-mediated phosphorylation and K48-specific polyubiquitination and protein stability

(A) Nuclear translocation assay of SPOP-deficient RAW264.7 cells that were reconstituted retrovirally with IRF1 WT or IRF1 Y109F.

(B) IP/ IB analysis of K48-ubiquitination of IRF1 using transfected HEK293T cells.

(C) IB analysis of HEK293T cells that were transfected with IRF1 wt or IRF1 Y109F followed by cycloheximide (CHX) treatment to block protein translation for indicated time points.

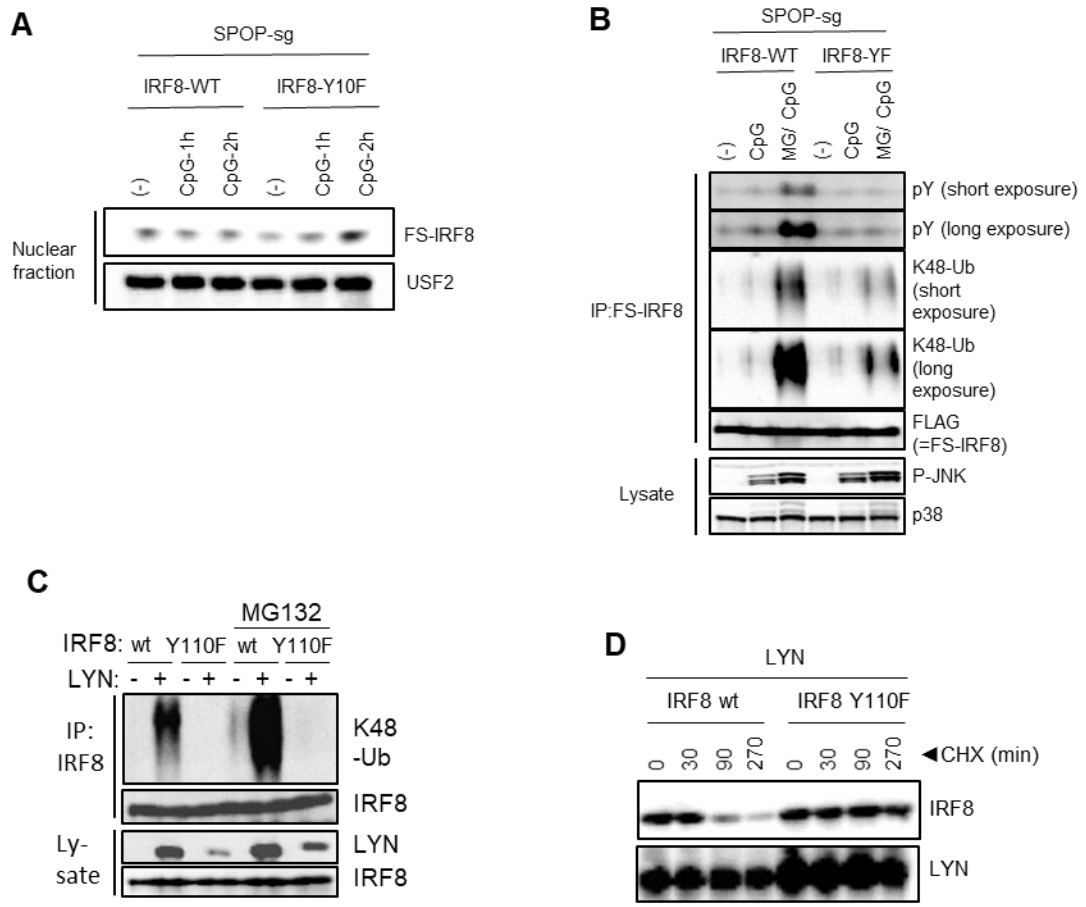

Fig. S6. A conserved tyrosine residue in IRF8 controls TLR-mediated phosphorylation and nuclear translocation.

(A) Nuclear translocation assay of SPOP-deficient RAW264.7 cells that were reconstituted retrovirally with IRF8 wt or IRF8 Y110F.

(B) IP/ IB analysis of IRF8 phosphorylation using cells described in (A). MG=MG-132.

(C) IP/ IB analysis of K48-ubiquitination of IRF8 using transfected HEK293T cells.

(D) IB analysis of HEK293T cells that were transfected with IRF8 wt or IRF8 Y110F, followed by cycloheximide (CHX) treatment to block protein translation for indicated time points.

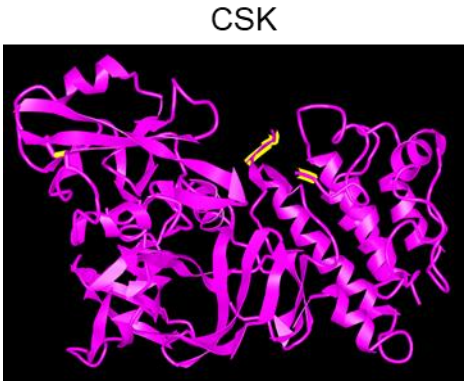

Fig. S7. The SPOP-binding motif in CSK is located in the kinase activation loop.
X-ray crystallography-based structure of CSK (PDB ID: 1K9A) with the SPOP-binding motif (EASST) in the activation loop highlighted in yellow (incompletely captured in crystal structure)(*64*).

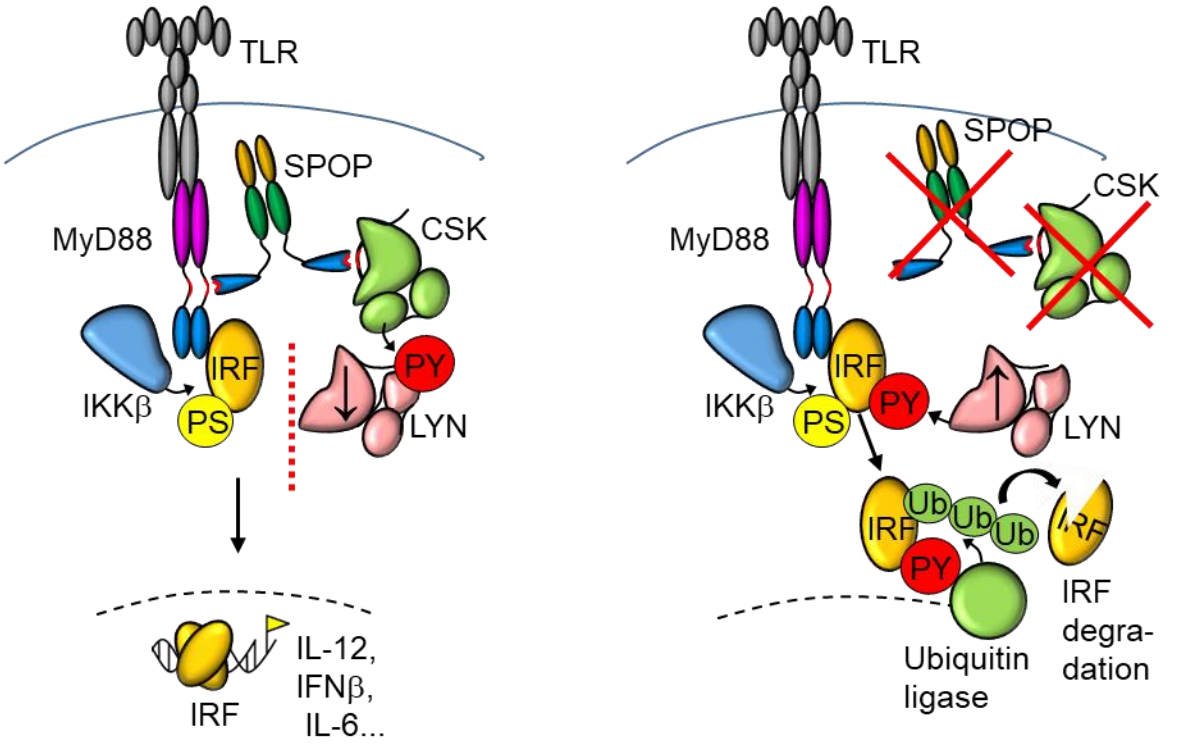

Physiological condition:
SPOP-mediated recruitment of CSK into TLR/ MyD88 signaling complex is critical to negatively control LYN, allowing nuclear IRF translocation and activation of target genes, such as type I interferons and IL-12

Interference with SPOP/ CSK:
Failure to contain LYN results in LYN-mediated phorphorylation of IRFs, leading to K48 polyubiquitination and degradation of IRFs and suppression of IRF-mediated gene transcription.

Fig. S8. Schematic model of signaling events controlling TLR-induced IRF activity.
PS, phosphoserine; PY, phosphotyrosine.